Sādhanā (2020)45:193
https://doi.org/10.1007/s12046-020-01441-y

© Indian Academy of Sciences

Determination of thermal performance of hydronic radiant panel heaters for different fluid flow rates, fluid inlet temperatures and room temperatures

TAMER CALISIR* and SENOL BASKAYA

Department of Mechanical Engineering, Gazi University, Ankara, Turkey
e-mail: tamercalisir@gazi.edu.tr; baskaya@gazi.edu.tr

MS received 31 December 2019; revised 3 April 2020; accepted 15 July 2020

Abstract. An experimental study of a commercially manufactured ceiling type hydronic radiant heating system has been performed in a test room, under controlled temperature conditions. One of the goals was to investigate how the radiant heater, under various operating conditions, affects the temperature distribution inside an occupied room. Another goal was to study the thermal performance of the radiant heating panel for different fluid inlet temperatures, fluid mass flow rates and test room temperatures. In addition, the temperature distribution on top of a surface placed below the heater, representing an actual application, was investigated. From the relevant literature, it was concluded that insufficient knowledge exists about these characteristics. The working fluid was water, and fluid inlet temperatures between 45 °C and 85 °C and mass flow rates of 97 kg/h and 174 kg/h were analyzed. The results showed that an almost linear increase in heat output arises, with the increase in the inlet water temperature. For lower inlet temperatures the heat output is moderately higher for a mass flow rate of $\dot{m}$ = 97 kg/h. The fraction of radiation heat transfer to the total heat transfer increases with decreasing water inlet temperature. It was also observed that, a relatively uniform temperature distribution could be obtained on the plate below the radiant panel. Furthermore, lower vertical temperature differences can be obtained inside the test room, for low water inlet temperature conditions. The obtained results of this study, could give information to manufacturers and building engineers, on the appropriate use and regulation of hydronic radiant systems.

Keywords. Radiant heating; ceiling radiant heater; heat transfer; radiation.

1. Introduction

Buildings are responsible for approximately one-third of global energy use, and have a high contribution to greenhouse gas emissions [1]. On the other hand, it is important to create a comfortable and healthy indoor environment in residential as well as large commercial buildings. Hence, due to the demand of decreasing the energy use in heating systems and less environmental pollution, the use of hydronic radiant systems, especially in commercial buildings, is becoming more popular day by day. Radiant heating systems can provide 50% or more of the total heat output, just by radiation. It was observed, that it is possible to obtain a high-energy efficiency using these types of radiant heating systems, due to the reduced distribution losses, and possibility of using low temperature water as the working fluid in various heating applications [2–4].

Radiant heating and cooling systems have been applied in residential as well as in non-residential buildings, such as offices, schools, airport terminals, railway stations, hospitals, manufacturing facilities [5, 6]. Hence, the interest has been growing nowadays for the heat transfer performance, and comfort conditions provided by the use of radiant panels.

Some experimental as well as CFD simulation studies have been performed, and can be found in the relevant literature. Tian and Love [1] investigated radiant slab cooling in a multi-floor building, through simulation and measured building energy use. Li *et al* [2] have built an experimental pilot project in a building where a radiant heating/cooling ceiling panel system was used, where they evaluated the performance of these systems. An experimental and numerical study was performed by Seyam *et al* [3] to investigate the performance of a radiant panel heating system, with regard to temperature and flow patterns inside the room. Koca and Çetin [7] and Koca *et al* [8] evaluated heat transfer coefficients and heat transfer characteristics of radiant heating systems. Wang *et al* [9] added holes to an existing radiant heating system, and experimentally evaluated the heat transfer of these systems. They set-up a

*For correspondence
Published online: 05 August 2020

radiant floor heating system, and its enhanced-convection type alternative in a climate chamber, and compared the results obtained from these systems. Yuan *et al* [10] developed new simplified correlations for the total heat transfer coefficient, and total heat flux density of radiant ceiling panels, which were proposed, based on experimental investigations. In another study performed by Yuan *et al* [11] information about some characteristics of radiant systems were presented, and the relationship between heat flux and surface temperature was analyzed. Roulet *et al* [12] used large panels to control the indoor temperature in several types of buildings. They showed that a small temperature difference between the panel and the indoor environment is sufficient to deliver and absorb the heat required.

A transient analysis has been performed experimentally and numerically by Fonseca [13], to evaluate the behavior of a hydronic ceiling system, and the interactions with its environment. In another study, Fonseca [14] presented the experimental procedure of a cooling ceiling system in a hospital room.

Energy consumption as well as comfort conditions are important parameters of radiant heating/cooling panels. Tye-Gingras and Gosselin [15] performed a hybrid numerical optimization study of ceiling and wall radiant panel systems in a residential building. The comfort and energy consumption of the system have been investigated. In an experimental and numerical study, Catalina *et al* [16] analyzed the indoor thermal comfort for a radiant ceiling cooling system, installed in a test room. Gemici [17] examined experimentally different radiant panel locations in a real size test chamber, and showed some thermal comfort aspects inside a room. Ali and Morsy [18] experimentally evaluated the ability of radiant panel heaters in producing thermal comfort, as well as energy consumption. They compared their results with conventional portable natural convective heaters.

Theoretical studies have also been performed for radiant heating systems inside various domains. Kuznetsov *et al* [19] investigated numerically the combined heat transfer by conduction, natural convection, and thermal radiation in an air-filled cavity with a radiant heater. Okamoto *et al* [20] developed a calculation method for estimating heat fluxes from ceiling radiant panels.

Leo Samuel *et al* [21] investigated the use of thermally activated building systems in a room using computational fluid dynamics (CFD) for different design parameters. The simulation results were used in obtaining thermal comfort indices.

The above discussion shows that there are some studies in the literature, which have focused on the subject of the heat transfer performance, and effect on thermal comfort of radiant heating/cooling systems. However, to the best knowledge of the authors, the use of a commercially manufactured ceiling type hydronic radiant heater inside a room, and the investigation of heat output and resulting temperature distribution inside the room under different operating conditions, has not been found in the literature. In all of the above presented investigations from the literature, the heating system consists of only a plane surface which is heated by various applications (e.g., electrical resistance heater), but do not resemble real commercial products (like piping system, insulation, radiant surface, etc.). In the present study, it was aimed to show the effects of a commercially manufactured hydronic radiant heater, on the temperature distribution inside an office room. In addition, another goal was to investigate the heating effects, of the applied ceiling type hydronic system, on a surface directly under the heater, representing a typical application. Furthermore, the performance of the system under various operating conditions was also analyzed. The findings of the present study could show, how the temperature distribution inside a room as well as a surface beneath the heater is being affected, by the use of a real heating application. Hence, the observations could guide in the effective use of commercially manufactured hydronic radiant heaters, under various working conditions.

2. Experimental study

2.1 *Test room description*

The experimental setup used in this study was installed inside a climatized and temperature controlled test room, with dimensions of 5 m × 4 m × 3 m. The schematic and real photos of the test room, hydronic radiant heater and measurement devices are shown in figure 1. As can be seen from figure 1(a) only the radiant panel has been placed inside the test room. All other heat-generating devices have been placed outside the test room. The radiant panel was placed in the center of the room, at a distance of 2.50 m from the bottom, according to EN 14037-2 [22]. The commercially manufactured hydronic radiant panel heater has a length of 2.0 m, a width of 1.5 m and a height of 0.05 m. The cross section of the heater has been presented in figure 1(b). The cross section in figure 1(b) shows that the water pipes are flush-mounted onto the heating surface. Heated water circulates inside the pipes and transfers its energy to the heating surface. The aim of the present study is to investigate the heat output of this system, and the effects on temperature distribution inside the room, as well as a plane surface underneath the radiator. Hence, an industrially used hydronic radiant heating system has been used. In these applications, the backside (side facing the ceiling) is insulated, in order to prevent heat loss through the backside of the radiant heater.

The circulation water temperature immediately before and after the radiant panel inlet/outlet sections, were measured with immersion type thermocouples as shown in figure 1. For the determination of the air temperature inside the room, 16 temperature measurement poles have been

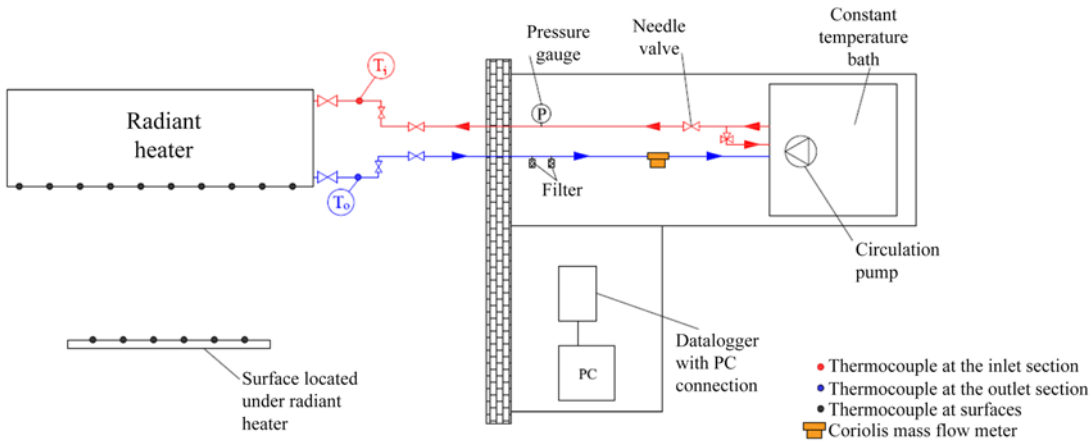

(a) Schematic of experimental set-up

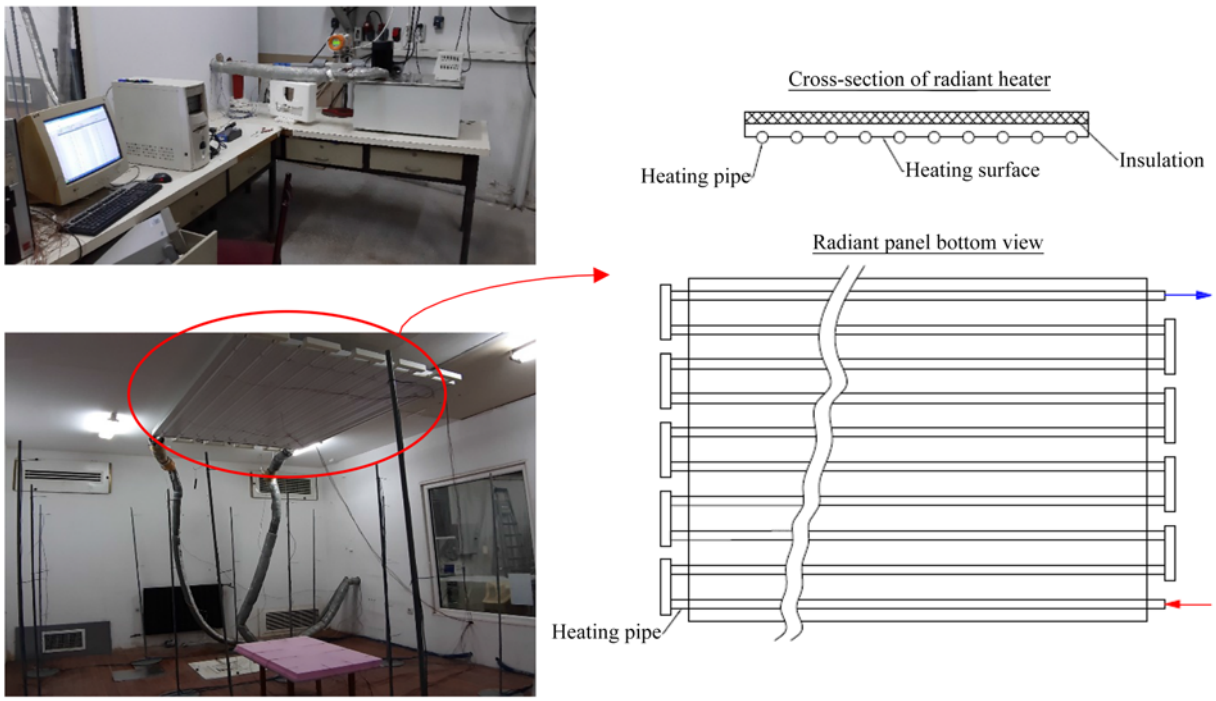

(b) Photos of the test room, measurement devices and cross section of radiant heater

Figure 1. Experimental set-up.

placed inside the test room. At all measurement poles four thermocouples were placed at heights of 0.10 m, 0.60 m, 1.10 m and 1.70 m. Hence, a total of 64 thermocouples have been used to track the temperature inside the test room. In addition, below the radiant heater, a surface with dimensions of 1.00 m × 0.60 m was placed at a height of 0.50 m from the floor. The height of 0.5 m signifies the knee height of a person, which is standing directly below the radiant heater. The aim was to show the heating effect below the heater, using a total of 16 thermocouples on this plane surface. In order to observe the effect by radiation heating, and prevent the effects of surface temperature on the measurement, an insulation material was used for this surface. A detailed description of the temperature measurement locations has been given in the next section.

2.2 *Measurement devices and measurement locations*

The heat input device was a constant temperature bath (LABO H541-D23) with a 3 kW immersion heater. Due to

a large water content in the bath, it was possible to keep the temperature steady throughout the experiments. The water flow rate was measured using a Coriolis mass flow meter (Kobold TME S80), with a measurement range of 0-600 kg/h, and an accuracy of ±0.4%. The mass flow meter was mounted at the return line of the radiant heater system. The circulation water was filtered using two different filters at the return line. Hot water was circulated using a pump, and the flow rate was controlled with a bypass-line and a needle valve (figure 1(b)).

The measurement of water inlet (T_i) and outlet (T_o) temperatures from the radiant heater have been performed by using immersion type thermocouples of type T, with a measurement range of − 200 °C–260 °C, and an accuracy of ±0.4%.

As can be seen from figure 2(a) thermocouples of type T (measurement range of − 200 °C–260 °C, accuracy of ±0.4%) were placed on the radiant heater, in order to measure the surface temperatures during the experiments. A total of 16 thermocouples were placed on the radiation surface of the hydronic heater. The thermocouples between T_{RH1}–T_{RH5} were placed on locations where the heating pipes are in contact with the radiation surface. The remaining thermocouples were placed on locations between the pipes.

Right below the radiant heater an insulation material surface has been placed, and 16 thermocouples (type T, measurement range of − 200 °C–260 °C, accuracy of ±0.4%) were mounted on this surface, in order to observe the heating effect of the radiant heater (figure 2(a)). These thermocouples have been named as T_P1–T_P16.

Figure 2(b) shows all 64 thermocouple locations inside the room. Thermocouples of type T (measurement range of − 73 °C–482 °C and accuracy of ±1.5%) were used, and were placed at heights of 0.10 m, 0.60 m, 1.10 m and 1.70 m. The locations and thermocouple numbers used to track the room temperature have been summarized in table 1.

Agilent 34970A model data logger, which was attached to a PC, was used to track and collect the temperature values. The temperatures of the radiant heater inlet and outlet were recorded as T_i (°C) and T_o (°C). All pipes connecting the constant temperature bath to the hydronic heater were well insulated. Hence, the only heat source in the test room was the radiant heater. The room was held at constant temperature using an air-handling unit, which delivers conditioned air to the room via four vents, as shown in in figure 2(b). The measured data was automatically recorded using BenchLink Datalogger 3 software at 30-second intervals.

2.3 *Experimental procedure*

The test room is located inside a large space where stable temperature conditions exist. Experiments were performed for water inlet temperatures of 45 °C, 55 °C, 65 °C, 75 °C and 85 °C. The effect of mass flow rate and room temperature on the heat output of the hydronic heater and temperature distributions on the above-explained surfaces, as well as inside the test room, were investigated. Tests were performed for room temperatures of 18 °C, 20 °C and 22 °C, which were adjusted using the air-conditioning system.

The inlet-outlet temperature values were used to calculate the heat output from the radiant heater. All experiments were performed under steady state test room and working fluid conditions. Therefore, the main consideration in the measurements was that all the temperatures reach steady state conditions. The steady state condition was checked by controlling the variation of all measured temperatures. These temperatures are the inlet/outlet temperatures of the radiant heater as well as the temperatures inside the room. After all these temperatures became constant, steady state conditions have been accepted as achieved. The time to reach steady state conditions was approximately 4 hours for an inlet temperature of 85 °C and mass flow rate of 174 kg/h. The time was shorter for the other operating conditions. However, in order to eliminate any possible unsteady effects, 4 hours were used in all experiments. After the establishment of steady state conditions, the actual data collection was continued for another hour. The measured data was automatically recorded using BenchLink Datalogger 3 software at 30-second intervals. The heat output from the radiant heater was determined using enthalpies related to the measured temperatures at the inlet and outlet sections.

3. Data reduction

3.1 *Determination of total heat output*

The total heat output of the radiant panel (Q_t) was calculated as shown in Eq. (1), where the difference of enthalpies between the inlet and outlet sections were used.

$$Q_t = \dot{m}\,(h_i - h_o) \tag{1}$$

where, $\dot{m}$ shows the mass flow rate (kg/s) of water, h_i and h_o are the enthalpies (J/kg) of water at the inlet and outlet ports, respectively. The enthalpies were obtained using thermodynamic tables at the respective temperature values [23].

According to EN 14037-2 [22] the water flow rate shall be regulated so that a Reynolds number value of Re = 4500±500 is achieved in the tubes of the ceiling mounted radiant panel at a water temperature of 50 °C. In addition, it is instructed that the mass flow rate shall be constant at each measuring temperature [22]. However, in order to show the effects of different operating

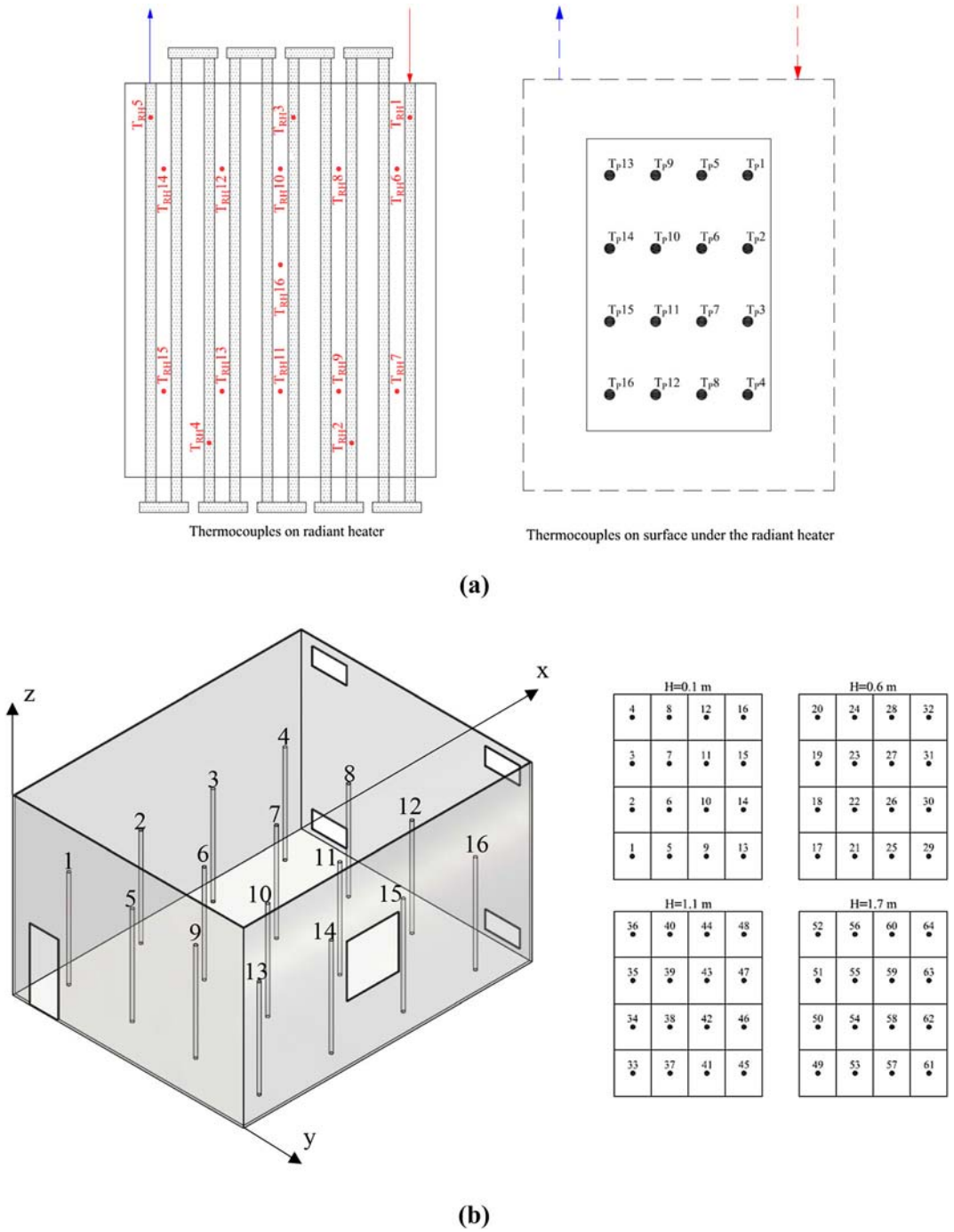

Figure 2. Temperature measurement locations. (a) measurement locations on panel and plate, (b) measurement locations inside the test room.

conditions on the heat output and temperature distribution inside the room and on the radiant panel surface, experiments were performed for two different Reynolds number values of Re = 2500 and Re = 4500. The mass flow rate was determined according to these Re numbers using the equation below.

$$\dot{m} = \frac{\mu.\pi.D.\mathrm{Re}}{4} \tag{2}$$

where, ṁ (kg/s) is the mass flow rate of water, μ (Pa.s) is the dynamic viscosity of water at 50 °C and D (m) is the inlet pipe diameter (25 mm) of the radiant panel. According

Table 1. Temperature measurement locations inside the test room.

	H = 0.1 m	H = 0.6 m	H = 1.1 m	H = 1.7 m
Location-1	1	17	33	49
Location-2	2	18	34	50
Location-3	3	19	35	51
Location-4	4	20	36	52
Location-5	5	21	37	53
Location-6	6	22	38	54
Location-7	7	23	39	55
Location-8	8	24	40	56
Location-9	9	25	41	57
Location-10	10	26	42	58
Location-11	11	27	43	59
Location-12	12	28	44	60
Location-13	13	29	45	61
Location-14	14	30	46	62
Location-15	15	31	47	63
Location-16	16	32	48	64

to these Re number values, the mass flow rates were obtained as 97 kg/h and 174 kg/h.

The radiative part of the heat output (Q_r – W) was calculated according to EN 14037-3 [24] using Eq. (3).

$$Q_r = \sigma.\varepsilon_{RH}.\left(T_{RH,m}^4 - T_a^4\right).A_{RH} \tag{3}$$

where, σ is the Stefan-Boltzmann constant (5.67×10^{-8} $W/m^2.K^4$), ε_{RH} emissivity of the radiant heater and A_{RH} is the area of the radiant heater surface facing the room. The emissivity was obtained from the manufacturer, and has a value of 0.93. The fourth power of the arithmetic mean surface temperature of the radiant heater ($T_{RH,m}$), and air temperature (T_a) obtained from the measurements were used, in the calculation of the radiative part of the total heat output. Although, EN 14037-3 [24] suggests to use wall temperatures in the calculation of the radiative part of the heat output, the air temperature has been used in the calculations in the present study. This was due to the long measurement periods used in the experiments. Hence, it was assumed that the wall temperatures are equal to the air temperature inside the room.

3.2 *Uncertainty analysis*

The accuracy of the experimental results was determined by performing an uncertainty analysis. The uncertainty in the experimental data was calculated according to the procedure proposed by Kline and McClintock [25], and Holman [26]. The uncertainty of variables were calculated using the root-sum-square formulation:

$$W_R = \left[\left(\frac{\partial R}{\partial x_1}W_1\right)^2 + \left(\frac{\partial R}{\partial x_2}W_2\right)^2 + \left(\frac{\partial R}{\partial x_3}W_3\right)^2 + \cdots + \left(\frac{\partial R}{\partial x_n}W_n\right)^2\right]^{1/2} \tag{4}$$

where R is the result of a given function of the independent variables x_1, x_2, x_3,…., x_n, w_R is the uncertainty of the variable R, and $W_i(W_1, W_2,\ldots., W_n)$ is the uncertainty of the independent variable. The uncertainty and possible errors in the determination of the total and radiative heat output and Re number were examined. The uncertainties of the dimensions of the radiant panel and thermo-physical properties of water were neglected in the calculations. It was observed that the highest uncertainty for the total heat output and radiative heat output have a value of approximately 4.15% and 2.20%, respectively.

4. Results and discussions

The experimentally obtained findings of this investigation have been presented in this part of the study, together with relevant discussions. In the present study, it was aimed to investigate the effects of various working conditions on the heat output of a ceiling type commercially manufactured hydronic radiant heater, and temperature distributions inside an office room, as well as, temperature distributions on a plane surface beneath the radiator.

The total heat output of the hydronic ceiling radiant panel has been obtained for different mass flow rates and water inlet temperature conditions. The effect of these parameters on the room temperature distributions as well as on the temperature distributions below the heater have also been examined. The application of a commercially manufactured radiant heater has been shown; hence, the results were presented in total heat output, instead of heat transfer per unit area.

The change in heat output with respect to inlet temperature for different mass flow rates and room temperatures has been shown on figure 3. The results shown in figure 3(a) were obtained for a constant room temperature of 20 °C. Whereas, results presented in figure 3(b) are for a constant mass flow rate of $\dot{m}$ = 174 kg/h. Experiments were performed for water inlet temperatures in the range of 45 °C – 85 °C. Error bands have been shown on the figures, in order to show the effects of measurement uncertainty.

With respect to figure 3(a), an almost linear increase in the heat output for both mass flow rates has been obtained. It was observed that, for lower inlet temperatures the heat output is moderately higher for a mass flow rate of $\dot{m}$ = 97 kg/h. However, with the increase of inlet temperature the heat output becomes higher for $\dot{m}$ = 174 kg/h. Nevertheless, the results show that for all investigated temperatures, except T_i = 45 °C, the variation is less than the

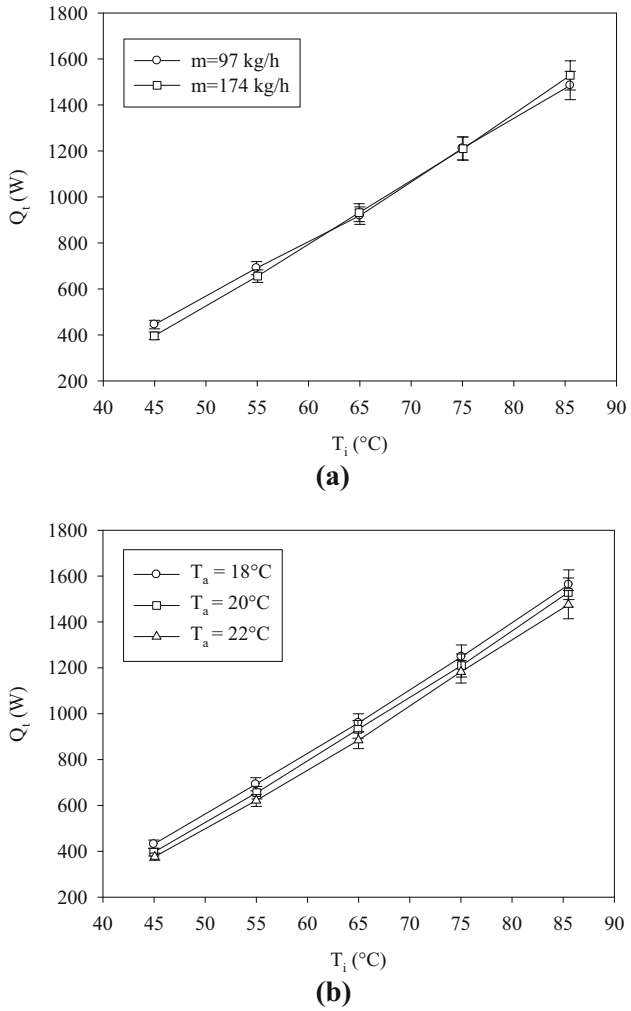

Figure 3. Heat output of hydronic radiant heater for different working conditions with changes in the inlet temperature (a) effect mass flow rate (T_a = 20 °C), (b) effect of room temperature ($\dot{m}$ = 174 kg/h).

measurement uncertainty. For an inlet temperature of 45 °C, an increase of almost 11% could be obtained. Although, there is a decrease of almost 44% in the mass flow rate, the decrease in temperature between the inlet and outlet sections, is only 9% for a mass flow rate of $\dot{m}$ = 97 kg/h. Whereas the decrease is only 4% for a mass flow rate of $\dot{m}$ = 174 kg/h. Due to this difference in the temperature drop between the inlet and outlet sections, a higher heat output can be obtained for low inlet temperatures and low mass flow rates. However, with the increase in inlet temperature the heat output is unaffected from the mass flow rate.

Risberg *et al* [27] reported that for panel radiators the heat output is almost unaffected for a mass flow rate above a certain value. Similar results were obtained in the present study, for the ceiling radiant heater.

The effect of the room temperature on the heat output has been examined for temperature values of 18 °C, 20 °C and 22 °C, and the results have been presented in figure 3(b). The room temperatures were obtained by calculating the arithmetic mean of the measurement results obtained by the thermocouples placed inside the room. Heat output results for different inlet temperature values are shown on figure 3(b). The results are in agreement with the findings of figure 3(a), and one can see that the heat output increases linearly with the increase in water inlet temperature. It was observed that with the decrease in room air temperature, the heat output of the radiant heater increases, which is due to the increase in the temperature difference. However, as can be seen from the error bars, the increase is within the experimental uncertainty. Hence, it can be concluded that the effect of room temperature on the heat output of the radiant heater can be neglected.

According to Eq. (1), the two main parameters affecting the total heat output of the radiator are the mass flow rate and difference of enthalpies between inlet and outlet sections. The difference of enthalpies is related to the temperature difference between the inlet and outlet sections. However, for a constant water inlet temperature the outlet temperature changes with the change in mass flow rate. For lower mass flow rates, the circulation water resides for a longer time inside the heater, and consequently a lower outlet temperature is achieved due to increased heat transfer. Hence, for lower mass flow rates the difference between the enthalpies increases in such a way that the change in mass flow rate has an insignificant effect on the total heat output.

In order to show the effect of temperature difference between the radiant heater inlet and outlet (ΔT), calculations were performed for different mass flow rates and inlet temperatures. The obtained results have been shown on figure 4. It was observed that, for $\dot{m}$ = 97 kg/h and T_i = 45

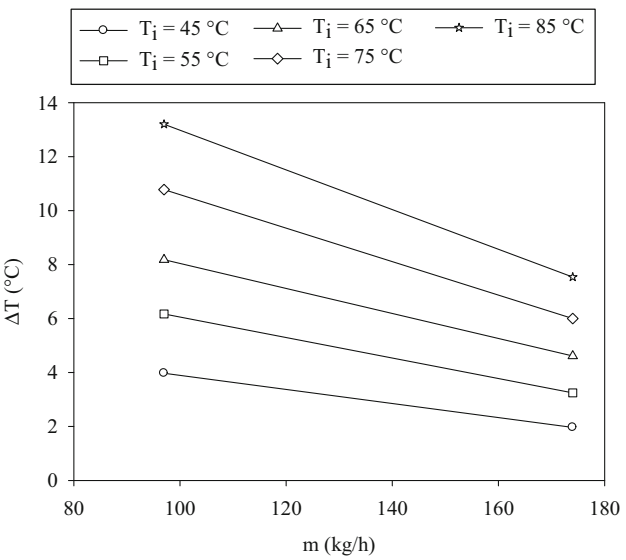

Figure 4. Change of temperature difference between inlet and outlet with mass flow rate for different inlet temperatures (T_a = 20 °C).

°C the temperature difference is approximately 4 °C, whereas for the same inlet temperature and $\dot{m}$ = 174 kg/h, the temperature difference drops to 2 °C. Although, there is an increase of almost 44% in mass flow rate, the change in the temperature difference is lower for an inlet temperature of 45 °C. Hence, the findings of figure 3(a) are in agreement with the findings of figure 4. As the inlet temperature increases, the magnitude of the slope of the temperature difference increases. A temperature difference of almost 13.2 °C is obtained for a mass flow rate of 97 kg/h and inlet temperature of 85 °C. A decrease of almost 43% occurs with the increase of mass rate to 174 kg/h, for the same inlet temperature. This is almost equal to the percentage increase of the mass flow rate. Hence, with the consideration of experimental uncertainty, it can be concluded that for $T_i \geq 55$ °C the effect of mass flow rate on heat output could be neglected. These findings are in agreement with figure 3, and explain the ineffectiveness of mass flow rate on heat output. In addition, due to the increase in the dwell time of the water inside the radiant heater with decreasing mass flow rate, an increase in the temperature difference occurs between the inlet/outlet ports. The increase in temperature difference and decrease in mass flow rate are compensating each other, and therefore the effect of mass flow rate on the total heat output can be neglected for $T_i \geq 55$ °C.

The main part of heat output of ceiling radiant heaters is obtained by radiation, and as mentioned before 50% or more of the heat output occurs by radiation [3]. Therefore, the radiative part of the total heat output has been calculated in the present study, and the fraction of radiative part to the total heat output has been obtained and presented in figure 5. Error bars have been added to the figures to show the measurement uncertainties. The effect of water mass flow rate (figure 5(a)) and room air temperature (figure 5(b)) on the fraction of Q_r/Q_t is presented for different water inlet temperatures.

As can be seen from figure 5, the fraction of radiation heat transfer to the total heat transfer decreases with increasing water inlet temperature. This is the case for both, different room temperatures as well as mass flow rates. The decrease in the radiative fraction of heat transfer with the increase in inlet temperature is due to the increasing effects of natural convection from the outer surfaces of the hydronic system facing the room surfaces. Due to the natural convection currents arising on these surfaces, the fraction of radiation decreases, whereas natural convection heat transfer increases. This is due to an increase in the temperature difference between the surfaces of the hydronic system and the room temperature. However, there is an exception for a mass flow rate of 97 kg/h, where the fraction of radiation heat transfer is almost constant, and around approximately 70% of the total heat output occurs by radiation. Considering the error bars, representing the measurement uncertainties, it can be seen that the results are almost within the measurement uncertainty range.

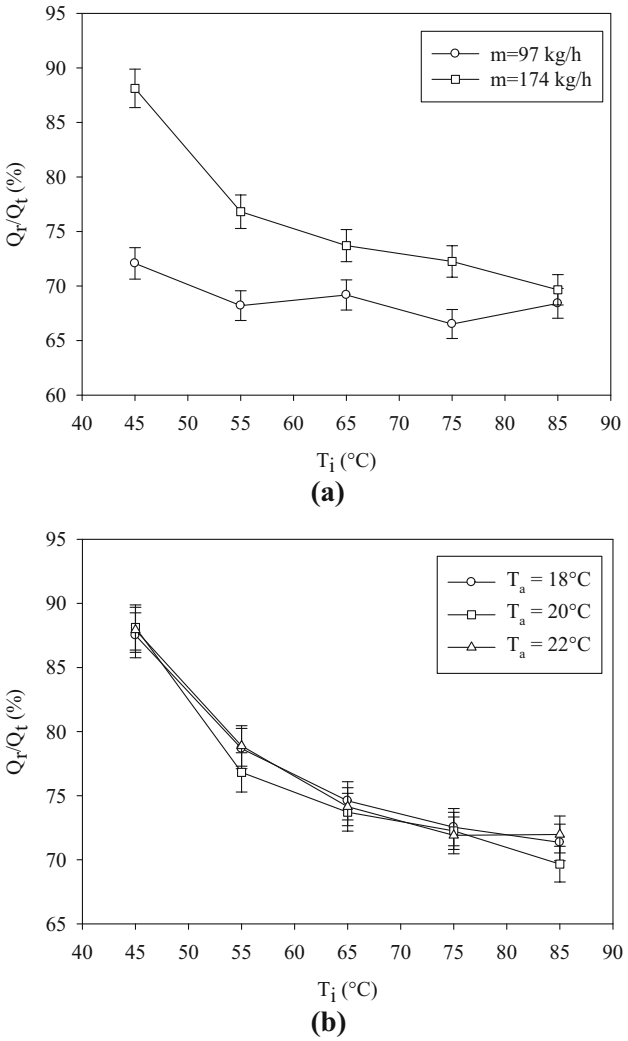

Figure 5. Fraction of heat transfer by radiation to the total heat output of the radiant panel (a) effect of mass flow rate (T_a = 20 °C), (b) effect of room temperature ($\dot{m}$ = 174 kg/h) with change in the inlet temperature.

Hence, it can be concluded that for a mass flow rate of 97 kg/h the fraction of radiation heat transfer is almost unaffected, by the change in the inlet temperature. Furthermore, from the findings by Dikmen [28], it was observed that with the decrease in the mass flow rate, the temperature distribution on the radiant panel becomes non-uniform. This is due to the lower velocity inside the pipes, which causes lower heat transfer coefficient values. Hence, the heat transfer from the pipes to the heating surface of the radiant heater decreases, causing a non-uniform temperature distribution.

In the study by Dikmen [28], CFD simulations have been performed for similar types of hydronic radiant heaters. In this study, it was reported that the velocity distribution around the radiant heater increases with the decrease in Re number, which has an increasing effect on convection. Therefore, the fraction of radiation heat transfer for lower

mass flow rates is lower, and for all inlet temperatures, an almost constant fraction of radiation heat transfer has been obtained.

For a water inlet temperature of 45 °C, the fraction of radiation heat transfer to the total heat transfer, is almost 88% for all room temperatures (figure 5(b)). In addition, the fraction of Q_r/Q_t is almost not affected by the room temperature. As can be seen from the figure, the differences are within the measurement uncertainties, which shows that the effect of room temperature on the fraction could be neglected.

On the other hand, the fraction of Q_r/Q_t is more affected by the water mass flow rate. In figure 3, it was observed that the total heat output is very close for the investigated range of mass flow rates. However, as can be seen from figure 5(a) the radiative part of heat transfer increases with the increase in mass flow rate. Especially, for a water inlet temperature of 45 °C, the fraction increases from 72% to 88%, with the increase in mass flow rate from 97 kg/h to 174 kg/h. The main expectancy of ceiling radiant heaters is to heat with radiation, particularly the occupants below the heater. Therefore, these findings show how the radiative part could be increased.

It was also observed that, for a mass flow rate of 174 kg/h, with the increase in inlet temperature, the radiative part of heat output decreases continually. For $\dot{m}$ = 97 kg/h and inlet temperature of 45 °C, the radiative part of the total heat output is approximately 72%, whereas for an inlet temperature of 85 °C this fraction was obtained as 68.4%, for the same mass flow rate. However, according to the measurement uncertainties shown on figure 5(a), it can be concluded that the results are within the measurement uncertainty, and the radiative fraction of heat transfer is almost unaffected, with the increase in inlet temperature at lower mass flow rates.

The surface temperature of the radiant heater is one of the main parameters affecting the radiative part of the total heat output. Hence, the radiant surface temperatures have been examined for different room temperatures and mass flow rates, and are shown on figure 6. The arithmetic mean temperatures presented have been calculated using the measurement results obtained on the radiant heater surface.

In figure 6(a), the effect of room temperature on the ceiling radiant heater arithmetic mean surface temperature ($T_{RH,m}$) has been presented. As can be seen, the surface temperature is almost not affected by the room temperature, and for all room temperatures, the arithmetic mean temperature increases linearly with the water inlet temperature. It was seen in figure 5(b), that the radiative part of the total heat output is also almost unaffected with the change in the room temperature. This can be interpreted with the findings of figure 6, where the surface temperature of the radiant heater does not change with the room temperature.

On the other hand, with the increase in the mass flow rate, the arithmetic mean surface temperature on the radiant heater increases (figure 6(b)). For both investigated mass

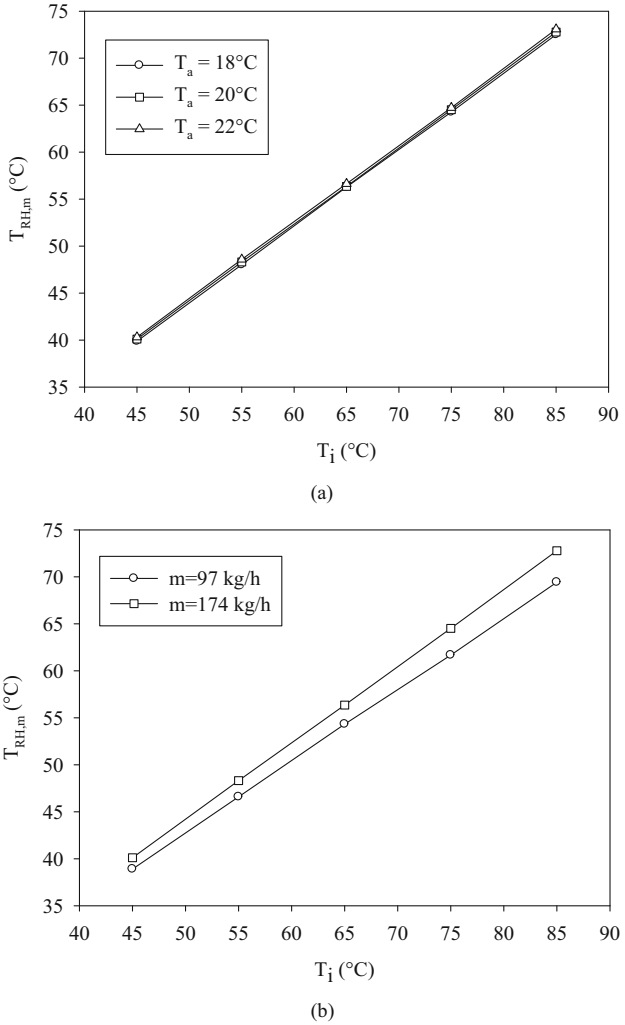

Figure 6. Effect of different operating conditions on radiant heater arithmetic mean surface temperature with changes in the inlet temperature (a) effect of room temperature ($\dot{m}$ = 174 kg/h), (b) effect of mass flow rate (T_a = 20 °C).

flow rates, the increase in the arithmetic mean radiant surface temperature occurs linearly with the increase in inlet water temperature. It was observed that, with the increase in the inlet temperature a slightly higher increase rate is obtained for a mass flow rate of 174 kg/h. Hence, for an inlet temperature of 45 °C, the difference is approximately 3%. However, this difference increases to approximately 4.50%, with the increase in the inlet temperature to 85 °C. With the increase in the water mass flow rate, the forced convection coefficient inside the pipes increases, which increases the heat transfer. Hence, the temperature values of the radiation surface increases, which in turn, at the same time, increases the arithmetic mean surface temperature.

In order to interpret the results of figure 6(b), the local temperature measurements where the heating pipes are in contact with the radiant panel (figure 2(a), $T_{RH}1$ – $T_{RH}5$)

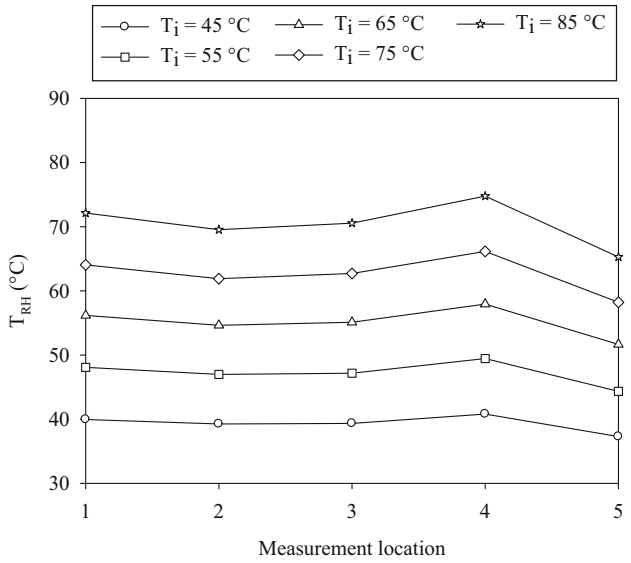

(a) ṁ=97 kg/h

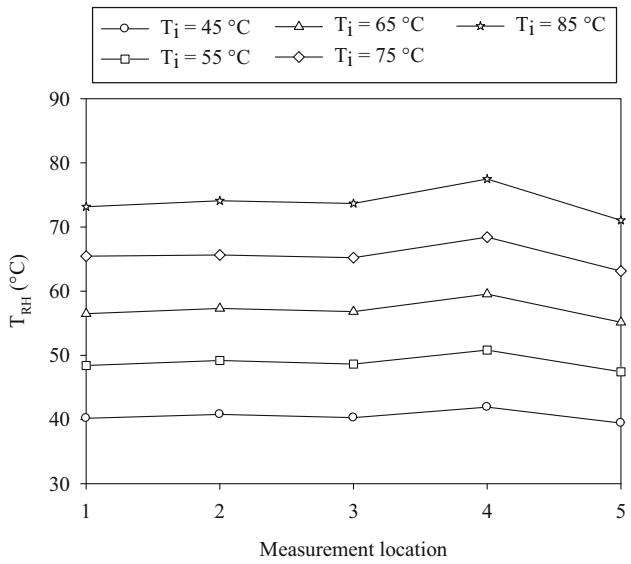

(b) ṁ=174 kg/h

Figure 7. Effect of mass flow rate on pipe surface temperature of radiant heater at different locations (T_a = 20 °C).

are shown on figure 7. The increase in the inlet temperature and mass flow rate increases the temperature values at these locations. This has an augmenting effect on the whole of the temperature distribution. Hence, the increase rate in the arithmetic mean temperature with inlet water temperature is higher as presented in figure 6. In addition, for a mass flow rate of ṁ = 174 kg/h a more uniform temperature distribution has been observed. These results are in agreement with Tye-Gingras and Gosselin [15], where it was reported that a reduction of the mass flow rate induces a larger temperature gradient on the heating panel. It was observed that a small increase in temperature occurs at $T_{RH}4$. Although, one would expect a temperature drop to occur at that location, it was seen that the temperature values are higher than at location $T_{RH}3$, for all investigated cases. The highest increase was calculated as around 2.5%, which is within the measurement uncertainty. However, from the findings of the CFD study performed by Dikmen [28], it was observed that the fluid velocity inside the pipes in that region increases, which moderately increases the temperature at the pipe. Hence, in the present study it was concluded that due to an increase in velocity inside the pipe a small increase in temperature occurs at $T_{RH}4$.

Another goal of this study was to observe the effect of the heating radiant panel on the temperature distribution inside the room, and especially below the radiant panel. Hence, this effect was examined for different mass flow rates and room temperatures.

In figure 8, the temperature distributions on the panel placed below the radiant heater, for different inlet temperatures and room temperatures have been presented. Compared to the findings shown before, the mass flow rate has a lower effect on the temperature distribution of the plate surface. As expected, the temperature on that surface increases with the increase in inlet temperature. For all investigated cases, it was observed that a relatively uniform temperature distribution occurs on the plate, which is a favorable characteristic of radiant heaters in actual applications.

It was also observed that, for a water inlet temperature of 45 °C, the arithmetic mean temperature on the plate of 21.4 °C was obtained, for both mass flow rates. With the increase in the inlet temperature, the arithmetic mean temperature on the plate also increases. For high temperatures, one can see some high temperature locations, which increase up to 26 °C. The plate was located at a height of 0.50 m. Hence, it could be interpreted that with the increase in height, the temperature values will increase under the radiant panel, for higher inlet temperatures.

The effect of room temperature has been examined in figure 8 (b). The results have been shown for different water inlet temperatures, and for a mass flow rate of ṁ = 174 kg/h. With the increase in room temperature, an increase in the temperature distribution on the plate occurs, for water inlet temperatures of 65 °C and 75 °C. On the other hand, for a room temperature of T_a = 18 °C, the lowest temperature occurs for an inlet temperature of 45 °C as 19.9 °C.

In order to show the effects of the use of the air-conditioning system and the radiant heater on the temperature distributions inside the test room, additional experiments have been performed. Experiments have been performed for the case when the radiant heater is not operating and operating. These results have been shown for T_a = 18 °C. For the operation of the radiant heater, experimental results were shown for a water inlet temperature of 45 °C and mass flow rate of ṁ = 174 kg/h. In addition, a comparison has

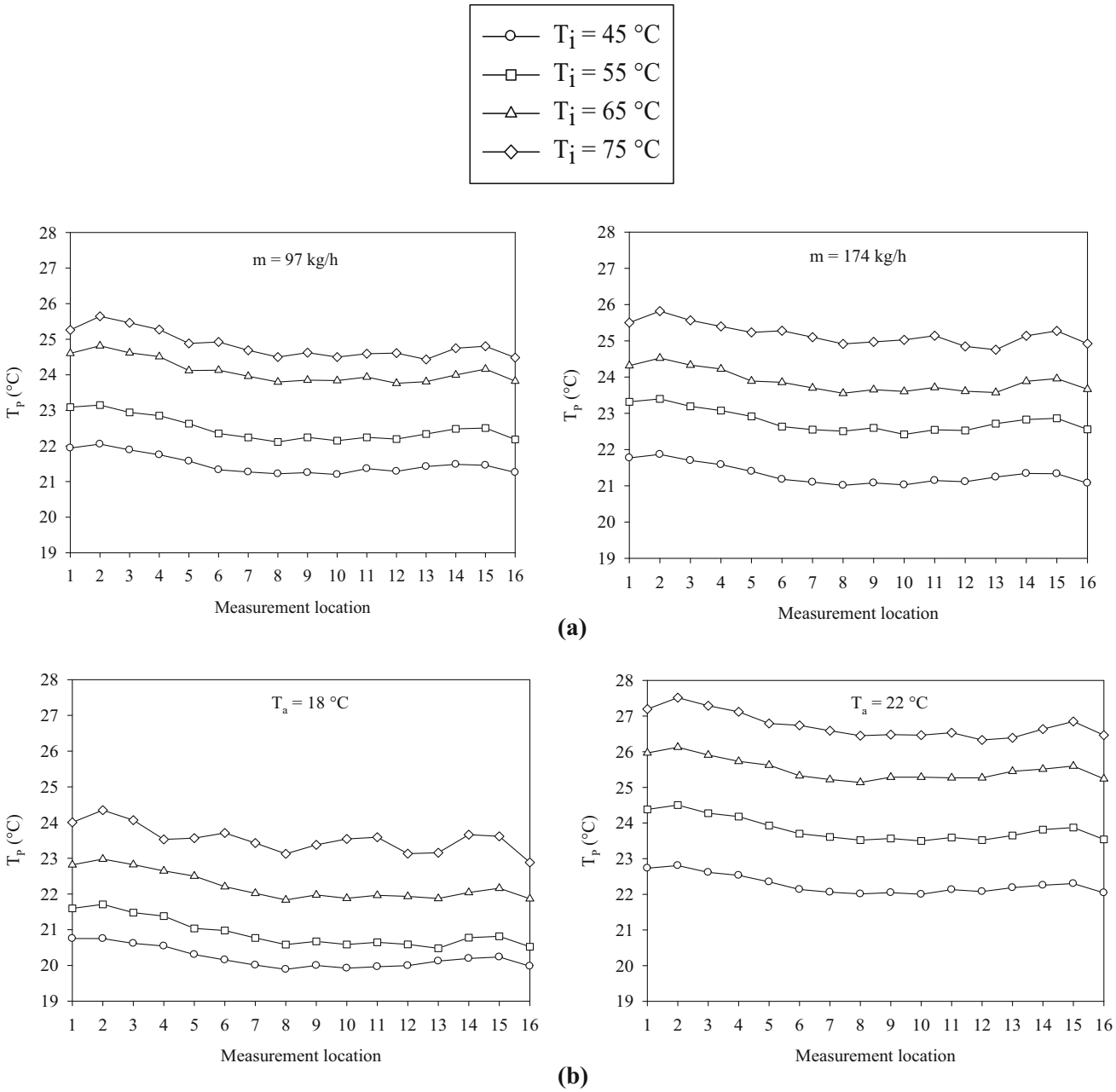

Figure 8. Local temperature distributions on the plate located below the radiant heater (a) effect of different mass flow rates (T_a = 20 °C), (b) effect of room temperature ($\dot{m}$ = 174 kg/h).

been performed, with and without the air-conditioning system under operation. The results have been presented for the case of $\dot{m}$ = 97 kg/h and T_i = 75 °C. With the air-conditioning system switched on, the room temperature was held at T_a = 18 °C. All these results have been summarized in table 2. The temperature values obtained at the 64 measurement locations (figure 2) has been presented and compared.

It was observed that, when the radiant heater is in use or not in use the temperature distributions are fairly close. As can be seen, the highest temperature difference is around 1.5 °C. In addition, the temperature also increases for higher elevations. In the central region of the room, the temperature values are slightly higher, due to the location of the radiant heater. For locations, which correspond to Location-6, Location-7, Location-10 and Location-11 (figure 2(b)), temperature differences of up to 1°C, compared to the other locations, have been obtained. At the mentioned locations, a temperature difference between the heights of H = 0.1 m and H = 1.7 m of approximately 4.0 °C was obtained for 45 °C water inlet temperature.

Table 2. Temperature distributions inside the room for different operating conditions.

Effect of radiant heater operation. (without operation – non RH, with operation – RH)

H = 0.1 m			H = 0.6 m			H = 1.1 m			H = 1.7 m		
T_a (°C)			T_a (°C)			T_a (°C)			T_a (°C)		
Loc.	*non RH*	*RH*	*Loc.*	*non RH*	*RH*	*Loc.*	*non RH*	*RH*	*Loc.*	*non RH*	*RH*
1	15.5	16.4	*17*	18.1	18.6	*33*	19.4	19.5	*49*	20.2	20.4
2	16.1	17.1	*18*	19.0	19.2	*34*	19.8	19.9	*50*	20.1	20.5
3	16.9	17.3	*19*	19.2	19.2	*35*	19.2	19.6	*51*	19.6	20.2
4	18.0	18.0	*20*	18.0	18.5	*36*	18.6	19.2	*52*	19.6	20.1
5	16.3	17.2	*21*	17.5	18.1	*37*	18.9	19.4	*53*	19.7	20.1
6	16.0	17.3	*22*	17.6	18.4	*38*	18.0	19.6	*54*	19.7	20.6
7	16.4	17.8	*23*	17.7	18.6	*39*	18.7	19.7	*55*	19.4	20.6
8	16.5	17.7	*24*	17.8	18.5	*40*	18.7	19.3	*56*	19.4	20.0
9	16.7	17.7	*25*	18.2	18.9	*41*	18.5	19.0	*57*	19.6	20.1
10	16.3	17.6	*26*	18.1	18.9	*42*	18.7	19.6	*58*	19.5	20.7
11	16.1	17.6	*27*	18.2	19.1	*43*	18.6	19.6	*59*	19.3	20.7
12	15.5	17.6	*28*	18.1	18.9	*44*	18.7	19.5	*60*	19.3	19.9
13	16.3	17.3	*29*	18.6	19.1	*45*	19.1	19.6	*61*	19.2	19.7
14	16.2	17.7	*30*	18.4	19.1	*46*	18.0	19.6	*62*	19.2	19.9
15	16.6	17.8	*31*	18.1	18.7	*47*	19.2	19.8	*63*	19.3	19.8
16	17.3	18.1	*32*	18.5	18.6	*48*	19.2	19.7	*64*	19.4	19.9

Effect of air-conditioning system. (without operation – non ACU, with operation – ACU)

H = 0.1 m			H = 0.6 m			H = 1.1 m			H = 1.7 m		
T_a (°C)			T_a (°C)			T_a (°C)			T_a (°C)		
Loc.	*non ACU*	*ACU*	*Loc.*	*non ACU*	*ACU*	*Loc.*	*non ACU*	*ACU*	*Loc.*	*non ACU*	*ACU*
1	16.7	16.3	*17*	18.8	17.5	*33*	19.7	18.7	*49*	20.5	19.5
2	17.6	16.3	*18*	19.2	17.9	*34*	20.2	19.0	*50*	21.0	20.0
3	16.5	15.1	*19*	19.1	18.1	*35*	20.2	19.1	*51*	20.9	19.8
4	16.8	15.5	*20*	18.8	17.8	*36*	19.6	18.5	*52*	20.6	19.5
5	17.6	17.4	*21*	18.5	17.2	*37*	19.8	18.7	*53*	20.7	19.7
6	18.3	17.3	*22*	19.2	18.1	*38*	20.2	19.2	*54*	21.6	20.6
7	18.6	17.5	*23*	19.3	18.3	*39*	20.5	19.5	*55*	21.7	20.7
8	18.3	17.0	*24*	19.1	18.1	*40*	19.8	18.7	*56*	20.5	19.4
9	18.3	18.1	*25*	19.4	18.1	*41*	19.4	18.3	*57*	20.6	19.5
10	18.3	18.1	*26*	19.8	18.3	*42*	20.4	19.3	*58*	22.0	20.7
11	19.0	17.4	*27*	19.7	18.6	*43*	20.6	19.4	*59*	22.2	21.1
12	19.5	19.3	*28*	19.2	18.5	*44*	20.3	19.2	*60*	20.5	19.4
13	17.8	17.2	*29*	19.4	18.3	*45*	19.9	18.7	*61*	20.0	19.0
14	18.6	17.2	*30*	19.8	18.5	*46*	20.1	19.0	*62*	20.3	19.3
15	18.2	16.9	*31*	19.2	18.1	*47*	20.5	19.3	*63*	20.3	19.3
16	17.2	16.9	*32*	19.2	18.2	*48*	20.4	19.2	*64*	20.3	19.3

The ISO 7730 standard [29] mentions the temperature difference between the ankle (H = 0.1 m) and head (H = 1.1 m) in the determination of percentage dissatisfied (PD). This is one of the comfort design criteria according to ISO 7730 [29]. Using the findings in table 2, the temperature differences between the elevations of H = 0.1 m and H = 1.1 m have been obtained as approximately 2.6 °C for 45 °C inlet temperature. This result shows a percentage dissatisfied (PD) of approximately 5%, according to ISO 7730 [29]. However, more data should be obtained in the ultimate determination of the thermal comfort inside a room [30].

In addition, experiments have been performed to show effects on the temperature distributions inside the room, for the case where the air-conditioning system is not used, while the hydronic system is operating. The results have

been presented in the lower part of table 2. A comparison has been performed, with and without the air-conditioning system under operation. The results have been presented for the case of $\dot{m}$ = 97 kg/h and T_i = 75 °C. The temperature results are fairly close, and showed that the air-conditioning system has almost no effect on the temperature distribution inside the room. In addition, it can be concluded that the temperature distribution is mainly affected by the radiant heater.

5. Conclusions

In this work, an experimental study was carried out to investigate the thermal heat output of a commercial ceiling type hydronic radiant panel heating system, for different water inlet temperature and mass flow rate conditions. In addition, the effects of water inlet temperatures and mass flow rates on the room temperature, as well as on the temperature distribution on a surface below the radiant heater were examined. The main goal of the present study was to investigate the temperature distributions inside an office room, as well as thermal performance of a commercially manufactured hydronic radiant heater. The outcomes obtained, should be able to guide the appropriate use and regulation of hydronic radiant systems. Hence, a real heating application was investigated experimentally. The thermal performance and temperature distributions inside the room, which have a direct effect on thermal comfort, have been presented. From the discussions presented above the following conclusions are be drawn.

- It was observed that the heat output is unaffected from the room temperature, and the obtained differences are within the measurement uncertainty.
- Except for the case of T_i = 45 °C, the heat output is also unaffected from the mass flow rate, because, the resulting differences are within the measurement uncertainty.
- For an inlet temperature of 45 °C, the heat output is higher for a mass flow rate of $\dot{m}$ = 97 kg/h, which is due to the high temperature drop between the inlet and outlet sections, compared to $\dot{m}$ = 174 kg/h.
- The fraction of radiation heat transfer generally decreases with the increase in inlet temperature, due to the increasing effect of natural convection currents on the surfaces of the hydronic system.
- However, for the mass flow rate of 97 kg/h, the fraction of radiation heat transfer is almost constant within the measurement uncertainty, and a fraction of around 70% has been obtained for all inlet temperatures.
- Due to a more uniform surface temperature obtained for higher mass flow rates, the fraction of the radiation heat output is almost 88% for an inlet temperature of 45 °C, and decreases continually with increasing inlet temperature, due to increasing natural convection effects.
- The fraction of radiation heat transfer is unaffected by the room temperature, and for all room temperatures the resulting differences are within the measurement uncertainty.
- There is no effect of room temperature on the radiant heater surface temperature.
- On the other hand, with increasing inlet temperatures the arithmetic mean temperature increases at a higher rate for higher mass flow rates.
- It was observed that, the mass flow rate has a low effect on the temperature distribution of the surface placed below the radiant heater, and the main parameter affecting the temperature distribution on this surface is the inlet temperature.
- For an inlet temperature of 45 °C, an arithmetic mean temperature of 21.4 °C was obtained on the surface below the radiant heater, whereas for higher inlet temperatures the mean temperature increases up to 26 °C.
- The vertical temperature differences decreases with the decrease in inlet temperature.
- In addition, the vertical temperature difference is considerably low for all cases, which is a favorable characteristic of these heating devices. Hence, the use of ceiling type hydronic radiant heaters in various occupied zones is very promising.

Acknowledgements

This research has been supported by the research fund of Gazi University under Grant No. BAP 06/2018-10. In addition, the authors also wish to thank NEOPLANT Ltd., Ankara, Turkey for the purchase and installation of the radiant heater.

Nomenclature

A	Area (m^2)
A_{RH}	Area of radiant heater radiation surface (m^2)
c_p	Specific heat (J/kg.K)
D	Diameter (m)
h	Enthalpy (J/kg)
k	heat conduction coefficient (W/m.K)
$\dot{m}$	mass flow rate (kg/s)
P	Surface temperature (°C)
Q	heat output of radiant panel (W)
Q_r	Radiative part of heat output (W)
Q_t	Total heat output (W)
Re	Reynolds number (−)
T	Temperature (°C)
T_a	Room air temperature (°C)
T_i	Water inlet temperature (°C)
T_o	Water outlet temperature (°C)
T_P	Surface temperature of plate below radiant heater (°C)
T_{RH}	Radiant heater surface temperature (°C)

$T_{RH,m}$ Radiant heater arithmetic mean surface temperature (°C)
x, y, z coordinates (−)

Greek symbols
Δ difference (−)
ε Emissivity (−)
μ Dynamic viscosity (kg/m.s)
ρ Density (kg/m^3)
σ Stefan-Boltzmann constant (W/m^2.K^4)

Subscripts and superscripts
a air
i inlet
m arithmetic mean
o outlet
p plate
RH radiant heater
r radiative
t total

References

[1] Tian Z and Love J A 2009 Energy performance optimization of radiant slab cooling using building simulation and field measurements. *Energy and Buildings* 41: 320–330

[2] Li R, Yoshidomi T, Ooka R and Olesen B W 2015 Field evaluation of performance of radiant heating/cooling ceiling panel system. *Energy and Buildings* 86: 58–65

[3] Seyam S, Huzayyin A, El-Batsh H and Nada S 2014 Experimental and numerical investigation of the radiant panel heating system using scale room model. *Energy and Buildings* 82: 130–141

[4] Rhee K N and Kim K W 2015 A 50 year review of basic and applied research in radiant heating and cooling systems for the built environment. *Building and Environment* 91: 166–190

[5] Rhee K N, Olesen B W and Kim K W 2017 Ten questions about radiant heating and cooling systems. *Building and Environment* 112: 367–381

[6] Dudkiewicz E, Jadwiszczak P and Jezowiecki J 2011 Examination of operational dynamics of radiant ceiling panel. *Central European Journal of Engineering* 1: 159–167

[7] Koca A and Çetin G 2017 Experimental investigation on the heat transfer coefficients of radiant heating systems: Wall, ceiling and wall-ceiling integration. *Energy and Buildings* 148: 311–326

[8] Koca A, Acikgoz O, Çebi A, Çetin G, Dalkilic A S and Wongwises S 2018 An experimental investigation devoted to determine heat transfer characteristics in a radiant ceiling heating system. *Heat and Mass Transfer* 54: 363–375

[9] Wang D, Wu C, Liu Y, Chen P and Liu J 2017 Experimental study on the thermal performance of an enhanced-convection overhead radiant floor heating system. *Energy and Buildings* 135: 233–243

[10] Yuan Y, Zhang X and Zhou X 2017 Simplified correlations for heat transfer coefficient and heat flux density of radiant ceiling panels. *Science and Technology for the Built Environment* 23: 251–263

[11] Yuan Y, Zhou X and Zhang X 2019 Numerical and experimental study on the characteristics of radiant ceiling systems. *Building Research & Information* 47: 912–927

[12] Roulet C A, Rossy J P and Roulet Y 1999 Using large radiant panels for indoor climate condition. *Energy and Buildings* 30: 121–126

[13] Fonseca N 2011 Experimental analysis and modeling of hydronic radiant ceiling panels using transient-state analysis. *International Journal of Refrigeration* 34: 958–967

[14] Fonseca N 2011 Experimental study of thermal condition in a room with hydronic cooling radiant surfaces. *International Journal of Refrigeration* 34: 686–695

[15] Tye-Gingras M and Gosselin L 2012 Comfort and energy consumption of hydronic heating radiant ceilings and walls based on CFD analysis. *Building and Environment* 54: 1–13

[16] Catalina T, Virgone J and Kuznik F 2009 Evaluation of thermal comfort using combined CFD and experimentation study in a test room equipped with a cooling ceiling. *Building and Environment* 44: 1740–1750

[17] Gemici Z 2017 Experimental examination of thermal comfort performance of a Radiant Wall Panel System: Comparison between Different Heating Wall Configurations. *J. Thermal Science and Technology* 37: 69–78

[18] Ali A H H and Morsy M G 2010 Energy efficiency and indoor thermal perception: a comparative study between radiant panel and portable convective heaters. *Energy Efficiency* 3: 283–301

[19] Kuznetsov G V, Kurilenko N I and Nee A E 2018 Mathematical modelling of conjugate heat transfer and fluid flow inside a domain with a radiant heating system. *International Journal of Thermal Sciences* 131: 27–39

[20] Okamoto S, Kitora H, Yamaguchi H and Oka T 2010 A simplified calculation method for estimating heat flux from ceiling radiant panels. *Energy and Buildings* 42: 29–33

[21] Leo Samuel D G, Shiva Nagendra S M and Maiya M P 2019 A sensitivity analysis of the design parameters for thermal comfort of thermally activated building system. *Sādhanā* 44: 48

[22] EN 14037-2, 2003 Ceiling mounted radiant panels supplied with water at temperature below 120 °C – Part 2: Test method for thermal output. European Committee for Standardization, Brussels, Belgium

[23] Cengel Y A and Boles M A 2006 *Thermodynamics: An Engineering Approach*, 5th edition. Boston: McGraw-Hill, 916–917

[24] EN 14037-3, 2003 Ceiling mounted radiant panels supplied with water at temperature below 120 °C – Part 3: Rating method and evaluation of radiant thermal output. European Committee for Standardization, Brussels, Belgium.

[25] Kline S J and McClintock F A 1953 Describing uncertainties in single-sample experiments. *Mechanical Engineering* 73: 3–8

[26] Holman J P 2011 *Experimental Methods for Engineers*, 8th edition. New York: McGraw-Hill, 63–70

[27] Risberg D, Risberg M and Westerlund L 2016 CFD modelling of radiators in buildings with user-defined functions. *Applied Thermal Engineering* 94: 266–273

[28] Dikmen T 2020 *Numerical Investigation of Ceiling Type Radiant Panel Heater*. M.Sc. Thesis, Gazi University, Ankara, Turkey

[29] EN ISO 7730 2005 Ergonomics of the thermal environment – Analytical determination and interpretation of thermal comfort using calculation of the PMV and PPD indices and local thermal comfort criteria. European Committee for Standardization, Brussels, Belgium

[30] Kumar Lachireddi G K, Muthukumar P and Subudhi S 2017 Thermal comfort analysis of hostels in National Institute of Technology Calicut, India. *Sādhanā* 42: 63–73